Bulletin of the New Zealand Society for Earthquake Engineering, Vol. 57, No. 1, March 2024

STRENGTHENING DAMAGED COLUMNS ON THE SOFT FIRST STORY OF REINFORCED CONCRETE BUILDING USING ULTRA-HIGH-STRENGTH FIBER-REINFORCED CONCRETE PANELS

Su A. Lim[1], Masanori Tani[2], Hidekazu Watanabe[3], Tomohisa Mukai[4], Eiichirou Nishimura[5], Shinsuke Hori[6], Tsubasa Hattori[7], Daisuke Matsumoto[8] and Minehiro Nishiyama[9]

(Submitted *November 2022*; Reviewed *April 2023*; Accepted *November 2023*)

ABSTRACT

In this study, ultra-high-strength fiber-reinforced concrete (UFC) panels were used as a quick and effective measure for seismic strengthening of damaged reinforced concrete (RC) columns. Four 1/3-scale specimens, which replicated RC columns of the soft-first-story of a 10-story condominium building that was heavily damaged in the 2016 Kumamoto Earthquake, were constructed and tested. The specimens were strengthened using UFC panels after being preloaded to the drift ratio, at which the maximum load capacity of the target column was measured, and then subjected to the main loading until the ultimate state was reached. The UFC panels were installed on the two faces of the column in a direction parallel to the assumed loading direction. Two of the specimens had a UFC or RC wing wall attached to one side of the column, which was also aligned with the assumed loading direction. During the preloading and main loading, the specimens were subjected to a cyclic lateral load and varying axial load that simulated an earthquake load. The proposed method improved the maximum strength and ultimate drift ratio, and helped restore the initial stiffness of specimens with UFC panels and a wing wall to that of a column specimen during preloading. The test results of a previous study, wherein the target column, loading method, and strengthening method were the same but the specimens were not damaged before strengthening, were compared to study the impact of the damage on the RC column before strengthening.

https://doi.org/10.5459/bnzsee.1627

INTRODUCTION

Earthquakes occur when the elastic stress caused by tectonic plate movement gradually accumulates, and when the fault zone rocks begin to fracture. The accumulated energy of the plate is released not all at once but several times. Several aftershocks are inevitable after the main earthquake, and these continuous quakes may cause secondary structural damage. In 2002, reinforcing bar buckling and concrete falling were witnessed in Molise, Italy, because of an aftershock of the same magnitude in a reinforced concrete (RC) structure that caused minor damage at the end of the column owing to the main earthquake of moment magnitude scale (Mw) 5.7 [1]. On April 14, 2016, a Mw 6.5 earthquake occurred in the Kumamoto region of Japan. In the subsequent aftershocks, a Mw 7.3 earthquake, which was stronger than the initial earthquake, occurred on April 16, followed by approximately 2000 aftershocks within a period of four months [2]. An earthquake with a magnitude equal to or greater than the first earthquake that occurred within a short period resulted in dozens of fatalities and severe structural damage to numerous buildings [3]. For instance, similar challenges in addressing neglected and partially demolished buildings have been observed in the aftermath of the 22 February 2011 earthquake in Christchurch, as documented in recent research [4]. Rapid seismic repair and retrofitting are required to reduce the cumulative damage caused by aftershocks and prevent further damage to structures.

Various studies are currently being conducted on the retrofit of damaged columns [5-9], and most of these studies propose fiber-reinforced polymer (FRP) sheets as a retrofitting method. The method utilizing FRP sheets involves adhering carbon fiber sheets to the surface of the structural member using epoxy resin. It has advantages such as lightweight, high tensile strength, and corrosion resistance. Consequently, it is being used for retrofit not only in columns [10-13] but also in beam-column joints [14-16], beams [17-19], and even bridge piers [20-22]. However, to achieve optimal performance in column retrofits, it is necessary to wrap all sides with fiber sheets. For square columns, sharp corners need to be chamfered to prevent the folding of carbon fibers. Additionally, care should be taken to avoid the formation of bubbles during the adhesive process, and multiple layers of FRP sheets may need to be applied for an effective retrofit. In some instances, a long construction period is required, which is unsuitable when rapid strengthening is necessary to prevent secondary damage to structures caused by continuous aftershocks following the initial earthquake.

This study proposes a rapid retrofit method using ultra-high-strength fiber-reinforced concrete (UFC) for an RC column. UFC is an extremely dense material composed of cement, ultrafine particles such as silica fume, and high-tensile strength

[1] *Corresponding Author, PhD, Kongju National University, Republic of Korea, sualim0126@gmail.com*
[2] *Associated Professor, Kyoto University, Kyoto, tani@archi.kyoto-u.ac.jp*
[3] *Senior Research Engineer, Building Research Institute, Tokyo, wata_h@kenken.go.jp*
[4] *Head, National Institute for Land and Infrastructure Management, Tokyo, mukai-t92ta@mlit.go.jp*
[5] *Chief Researcher, Toda Corporation, Tokyo, eiichirou.nishimura@toda.co.jp*
[6] *Group Manager, Maeda Corporation, Tokyo, hori.sin@jcity.maeda.co.jp*
[7] *Researcher, Kumagai Gumi Construction Company, Tokyo, tsubasa.hattori@ku.kumagaigumi.co.jp*
[8] *Research Engineer, Hazama Ando Corporation, Tokyo, matsumoto.daisuke@ad-hzm.co.jp*
[9] *Professor, Kyoto University, Kyoto, nishiyama.minehiro.8a@kyoto-u.ac.jp*

steel fibers. UFC has a higher compressive strength than 180 N/mm^2 and a higher tensile strength and ductility than plain concrete because of the fibers [23, 24]. Quick and easy strengthening of a column with insufficient residual seismic performance, such as lateral resisting or vertical load carrying capacity, can be achieved by applying an epoxy resin adhesive and attaching panels made of UFC.

Kumabe et al. performed a cyclic loading test on a column in the soft first story of a RC structure that was severely damaged in the 2016 Kumamoto Earthquake [25]. A 1/2-scale specimen was used as the target column, and flat UFC panels were adhered to the two pairs of opposite sides of the column using an epoxy resin adhesive to strengthen the target column. The level of damage to the column during preliminary loading was the main experimental parameter, and it was adjusted by preloading up to 0.5% and 3% of the specimen's drift ratio, respectively. The specimen's maximum strength was measured at a drift ratio of 0.5% of the preloading, and its damage condition corresponds to damage class III in Table 1, which is specified in the Japanese guidelines [26, 27]. The specimen that was loaded with a drift ratio of up to 3% before strengthening exhibited significant strength deterioration corresponding to damage class V in Table 1. The maximum strength of the specimen preloaded up to a drift ratio of 3% and retrofitted was 74% of the maximum strength before strengthening. Mortar patching with wet-spraying process and the strengthening method using UFC panels did not have a significant impact on the recovery of strength. In contrast, the specimen that was strengthened using UFC panels after loading up to a 0.5% drift ratio exhibited a maximum strength that was greater by a factor of 1.14 during preliminary loading, confirming the retrofitting effect of the UFC panels. Although the retrofitting effect could be confirmed for some specimens, all specimens exhibited joint mortar damage, such as crushing, between the stub and the UFC panel. As a result, the stress transfer between the stub and the UFC panel was reduced, and the UFC panel could not exert its maximum strength. Thus, the experiment was terminated prematurely.

The authors conducted a cyclic loading test by fabricating the same target column as five 1/3-scale specimens, including the non-strengthened specimen (target specimen) [28]. Figure 1 depicts the strengthening methods. The UFC sandwich panels were attached to the column, and there are two vertical cross-section types of the UFC panel. First, the thickness of both ends of the panel was twice that of the middle to reduce the effect of the joint mortar's damage on the maximum load capacity of the specimen. The second was the cross-section, wherein the joint mortar was removed and the UFC panel was bonded to the column with an epoxy resin adhesive and post-installed anchor.

Table 1: Damage class definitions of RC members [27].

Damage class	Description of damage
I	Visible narrow cracks on concrete surface (crack width is less than 0.2 mm)
II	Visible clear cracks on concrete surface (crack width is about 0.2–1.0 mm)
III	Local crush of concrete cover Remarkable wide cracks (crack width is approximately 1.0–2.0 mm)
IV	Remarkable crush of concrete with exposed reinforcing bars Spalling off of concrete cover (crack width is more than 2.0 mm)
V	Buckling of reinforcing bars Cracks in core concrete Visible vertical and/or lateral deformation in columns and/or walls Visible settlement and/or leaning of the building

Two of the specimens had a wing wall on one side of the specimen strengthened with UFC sandwich panels. There were two types of wing walls—UFC and RC. The maximum strength of the strengthened specimen was increased by 1.33 to 1.88 times, the ultimate drift ratio by 2 to 3 times, and the initial stiffness by 1.23 to 3.24 times compared to the target specimen.

This paper presents the cyclic loading test on our 1/3-scale specimens of the same target column as those in previous studies. The purpose of the study was to investigate the effectiveness of the strengthening method using UFC panels for damaged columns. The target column, loading method, and four retrofitting methods using UFC panels were the same as those in the previous study [28], but the specimens were damaged before strengthening. In the previous study conducted by Kumabe et al. [25], wherein the impact of the strengthening method using flat UFC panels on a damaged column was studied, the specimen that was strengthened using UFC panels after preloading up to a drift ratio of 0.5% exhibited increased strength. In this study, the specimen was strengthened using UFC panels after being preloaded to a drift ratio of 0.5% and then subjected to the main loading up to the ultimate state. The evaluation and comparison of the strength of each specimen, as well as the evaluation of the effect of damage caused by preloading, are discussed.

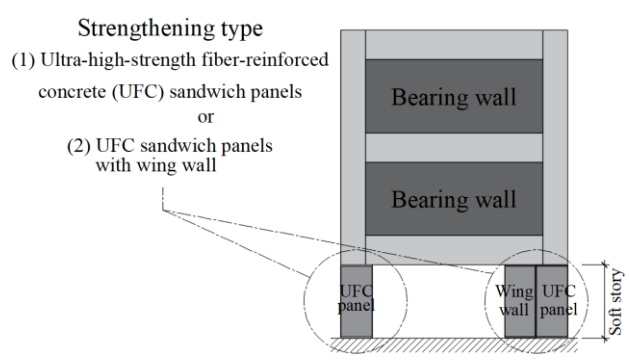

(a) Soft first story strengthened with UFC panels

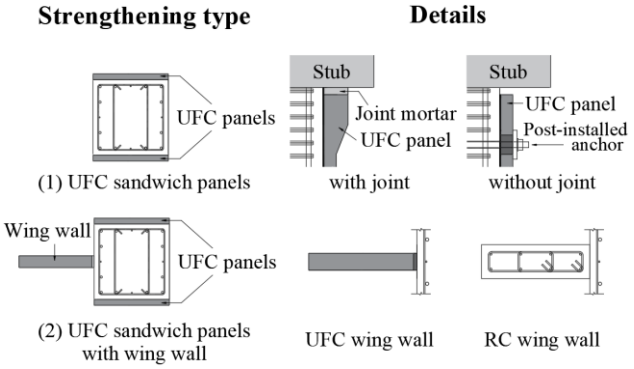

(b) Strengthening type in details

Figure 1: Proposed strengthening methods [28].

EXPERIMENTAL STUDY

Specimen Description

A column on the soft first story of the RC building that was severely damaged in the Kumamoto Earthquake was used as the target of the strengthening method using UFC panels proposed in this study. In the target column, the volumes of shear reinforcement in the X and Y directions differed significantly, and the crossties did not constrain the entire longitudinal rebar. As a result, shear failure occurred in the target column owing to the Kumamoto Earthquake, and the damage was classified as V in Table 1, indicating that it almost lost its lateral and vertical strengths.

Four identical specimens were produced for the cyclic loading test, as shown in Figure 2. The area from the first floor at ground level to the bottom of the beam on the second floor of the target building was scaled down by a factor of 1/3. The design compressive strength of the concrete was 35 N/mm^2 because the average of eight core samples taken from the first story on the target building was 35.4 N/mm^2. One specimen, strengthened with UFC sandwich panels and joint mortar injected between the UFC panel and the stub, was cast all at once. The remaining specimens were cast three times: lower stub, column section, and upper stub. Details are provided in [28].

The specimens were subjected to repeated cyclic loading as a preload up to a drift ratio of 0.5%, which represented the target specimen's maximum strength. After the specimens were damaged by preloading, the UFC panels were attached to two opposite sides of the column, with or without a wing wall on one side, as shown in Figure 3. Table 2 lists the strengthened specimens, where "-M" indicates preloading up to the drift ratio at which the target specimen's maximum strength was measured.

The UFC panels of all specimens were adhered with epoxy resin adhesive. C-US-M was the only one with post-installed chemical anchors, and it helped the force transfer between the column and the panels. High-strength and non-shrinkage mortar was injected into the holes of UFC panels for the anchor bolts, and once it hardened, a 40-Nm torque was applied to tighten the anchor bolt. The joints of the other specimens were filled with high-strength and non-shrinkage mortar at both the top and bottom ends of the panels, and the thickness of the ends of the panels was set such that it was double the value of thickness of the middle portion to prevent stress concentration. For the specimens with a wing wall, the column part was identical to that of C-USJ-M. The UFC wing wall was attached to one side of the column in C-USJ-UW-M using an epoxy resin adhesive. In addition, the upper and lower ends of the UFC wing wall were injected with high-strength and non-shrinkage mortar. C-USJ-RCW-M had the RC wing wall on one side of the column

Table 2: List of specimens.

C-US-M	Column - UFC Sandwich panels - Maximum load capacity
C-USJ-M	Column - UFC Sandwich panels with Joint mortar - Maximum load capacity
C-USJ-UW-M	Column - USJ - UFC Wing wall - Maximum load capacity
C-USJ-RCW-M	Column - USJ - RC Wing wall - Maximum load capacity

strengthened with UFC panels. The reinforcing bars of the RC wing wall were not anchored to the columns and stubs. The concrete was cast in place. For constructability, the upper 100 mm of the RC wing wall was filled with high-flow and non-shrinkage mortar. Table 3 presents the material test results for the strengthened specimens.

Loading Method and Sequence

The purpose of this study was to investigate the impact of strengthening with the UFC panel based on whether the target column is damaged before retrofit; the loading method was the same as that in the previous study [28]. An elevation view of the loading device is depicted in Figure 4, where the axial force was applied by two 8000-kN vertical jacks and the lateral force was applied by a 3000-kN horizontal jack. The loading in the south direction was positive. As depicted in Figure 5, all the specimens were subjected to varying axial forces to emulate the force applied to the column on the soft first story of the RC structure during an earthquake. The solid red line in the figure represents the axial force path of C-US-M; the black dashed line and solid black line indicate the shear force at the specimen's ultimate flexural strength Q_{mu} [30] and the ultimate shear strength Q_{su}, respectively [30]. The long-term axial force, N_0, at the point where the horizontal force was zero, was $0.15bDf'_c$ (b: width of the column, mm, D: depth of the column, mm, f'_c: compressive strength of the concrete, N/mm^2). The minimum axial force for tension was $-0.75A_g\sigma_y$ (A_g: gross cross-sectional area of the longitudinal bars of the column, mm^2, σ_y: yield strength, N/mm^2). The maximum axial force for compression was $0.40bDf'_c$. The axial force was linearly increased or decreased with the lateral force from the long-term axial force to the maximum axial force for compression or minimum axial force for tension, respectively. When the lateral force reached $Q_{su}/2$ under axial compressive force or $Q_{mu}/2$ under axial tensile force, the axial force was maintained at the target axial force, and the lateral force was applied until the target drift ratio was reached. In addition, the concrete compressive strength f'_c at the time of preloading was applied to determine the loading path for preloading and main loading.

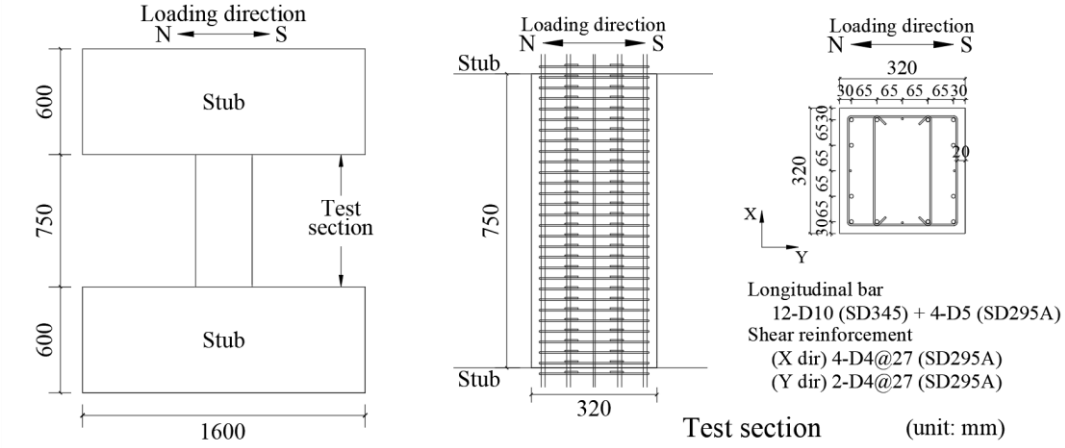

Figure 2: Overview of the target specimen.

(a)
C-US-M

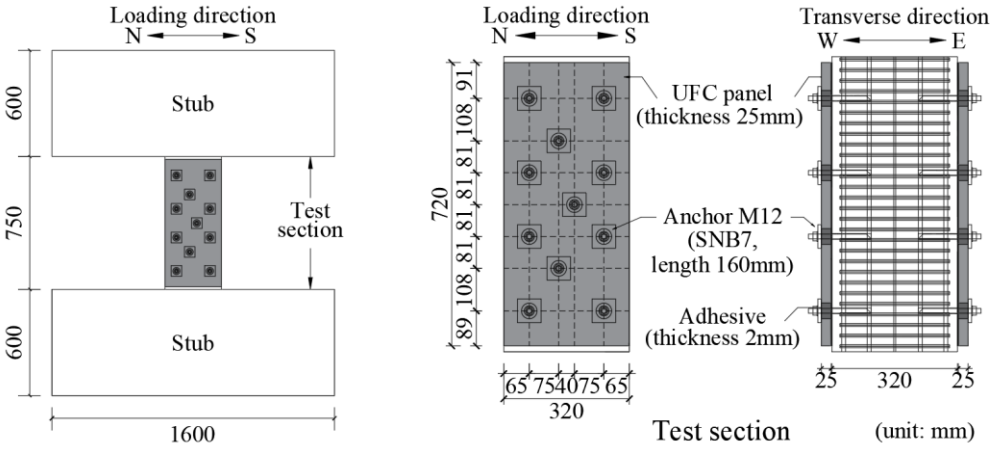

(b)
C-USJ-M

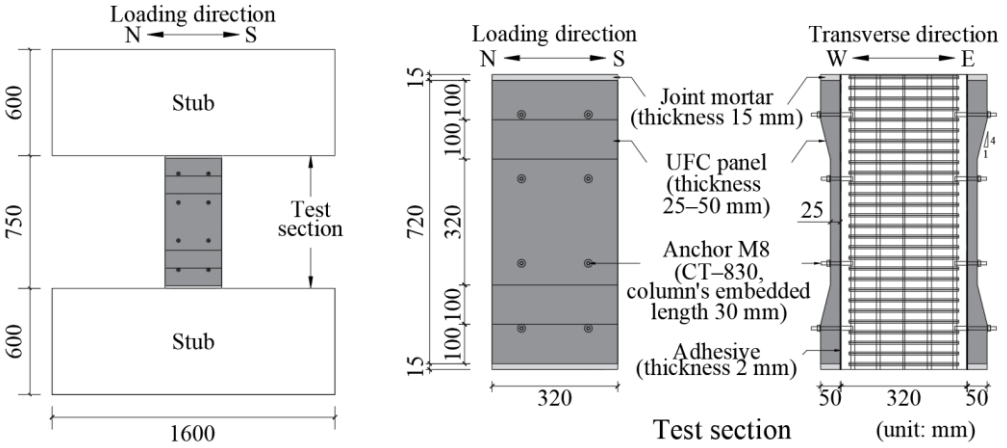

(c)
C-USJ-UW-M

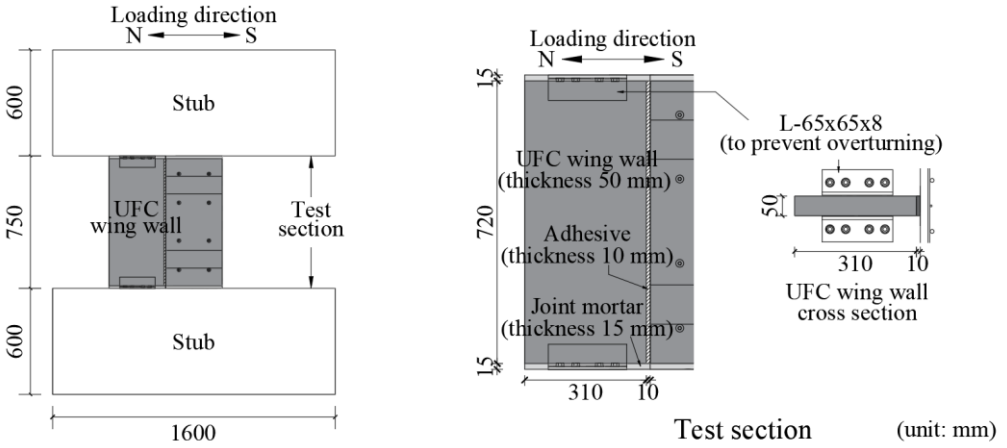

(d)
C-USJ-RCW-M

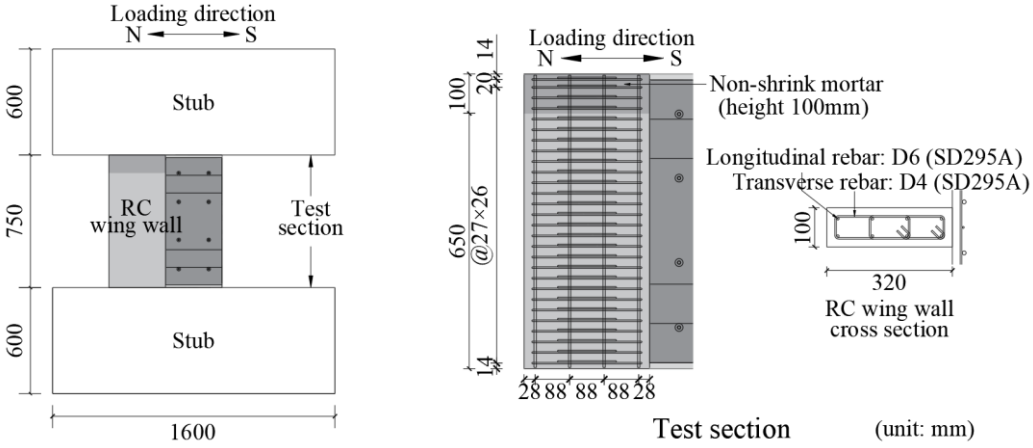

Figure 3: Overview of strengthened specimens (C-US-M: column-UFC sandwich panels; C-USJ-M: column-UFC sandwich panels with joints; C-USJ-UW-M: C-USJ-UFC wing wall; C-USJ-RCW-M: C-USJ-RC wing wall).

Table 3: Material test results.

(1) Concrete

Specimen	Loading stage	Age (day)	Compressive strength (N/mm^2)	Strain at compressive strength (%)	Elastic modulus (kN/mm^2)	Split tensile strength (N/mm^2)
C-US-M	Preliminary	153	48.7	0.260	28.7	3.1
	Main	238	48.1	0.224	28.6	2.9
C-USJ-M	Preliminary	124	40.7	0.232	27.0	3.1
	Main	174	40.7	0.229	27.0	2.7
C-USJ-UW-M	Preliminary	174	49.0	0.256	28.8	3.1
	Main	246	48.6	0.253	28.7	2.7
C-USJ-RCW-M	Preliminary	145	48.4	0.250	28.6	2.7
	Main	259 (42)*[1]	51.9 (47.4)*[1]	0.286 (0.311)*[1]	29.3 (28.5)*[1]	3.2 (3.3)*[1]

(2) Reinforcing bar

Type (steel type)	Location	Yield strength (N/mm^2)	Elastic modulus (kN/mm^2)	Tensile strength (N/mm^2)
D10 (SD345)	Column longitudinal	368.4	188.4	545.7
D5 (SD295A)		380.5*[2]	193.7	516.3
D4 (SD295A)	Column hoop	361.2*[2]	194.9	518.9
	RC wing wall transversal	347.0*[2]	193.5	513.2
D6 (SD295A)	RC wing wall longitudinal	475.8*[2]	192.6	564.4

(3) Mortar

Specimen	Location	Compressive strength (N/mm^2)	Specimen	Location	Compressive strength (N/mm^2)	Elastic modulus (kN/mm^2)
C-USJ-M	Joint	122.5 (40)*[3]	C-USJ-RCW	Joint	108.2 (57)*[3]	-
C-USJ-UW-M		129.1 (44)*[3]		RC wing wall	62.7 (40)*[3]	23.5

(4) Fiber in the UFC

Specimen	Density (g/mm^3)	Tensile strength (N/mm^2)	Diameter (mm)	Length (mm)
All specimen	7.8×10^{-3}	2.9×10^3	0.22	15.1

(5) UFC

	Compressive strength (N/mm^2)	Elastic modulus (kN/mm^2)	Flexural strength (N/mm^2)	Direct tensile strength (N/mm^2)
All specimen	216	52.9	60.6	22.8*[4]

**[1] ( ) is concrete of RC wing wall, *[2] 0.2% offset strength, *[3] ( ) is age (day), *[4] is calculated using Eq. (1)*

$$_{UFC}f_b = 2.59\,_{UFC}f_t + 1.54 \quad (1)$$

where $_{UFC}f_b$ = flexural strength of UFC obtained from a bending test (N/mm^2); and $_{UFC}f_t$ = direct tensile strength of UFC (N/mm^2) [27].

The drift ratio R is calculated by dividing the relative horizontal displacement of the upper and lower stubs by the clear height of the column. After preliminary cyclic loading, the specimens were strengthened using the UFC panel, and the main cyclic loading was performed thereafter to attain the specimen's ultimate state. The preliminary cyclic loading was conducted up to a drift ratio of 0.5%, and at this point, the maximum strength of the target specimen was reached [28]. Under the preliminary cyclic loading, one cycle was applied to the drift ratio R = 0.03125%, and two cycles were repeatedly applied to R = 0.0625%, 0.125%, 0.25%, and 0.5%, respectively. The main cyclic loading was conducted in the same manner as that in the preliminary cyclic loading, and R = 1%, 2%, 3%, and 4% were loaded repeatedly in two cycles, respectively. A pushover load was performed for the specimen that did not reach the ultimate state even after R = 4%.

Lateral Load–Drift Ratio Relationship and Damage Progress

Figure 6 shows the damage condition at the end of the preliminary loading of C-US-M and that at the end of the main

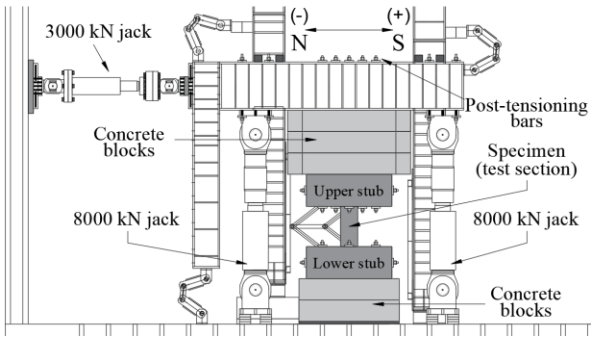

Figure 4: Loading setup (west side).

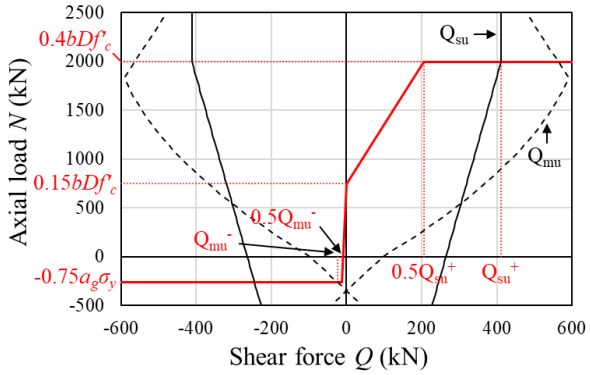

Figure 5: Axial loading path (C-US-M).

loading of each specimen. Figure 7 illustrates the lateral load–drift ratio relationship of C-US-M during preloading and the lateral load–drift ratio relationships of all the specimens during the main loading. The dashed line extended obliquely from the positive maximum strength point indicates the strength reduction due to the P–Δ effect. The ultimate drift ratio was set as the point where the load after the maximum strength decreased to 80% of the maximum strength. Cases where the longitudinal bar or shear reinforcement of the specimen yielded under the preliminary loading are excluded in the graph of the main loading.

Preliminary Loading

All specimens exhibited flexural tensile cracks throughout the column during the R = –0.03125% cycle. During the cycles with R = 0.125% or R = 0.25%, the longitudinal bars yielded in tension and compression. All specimens reached their respective positive and negative maximum yield strength during the cycle with R = 0.5%, as depicted in Figure 7(a). In addition, shear cracks occurred, and the shear reinforcement yielded in tension. Table 4 indicates the maximum strength for the positive loading direction during the preloading of each specimen. Although these values varied according to the difference in material strengths of the specimens, the differences were small. Among all cracks that occurred in each specimen at the end of the preliminary loading, the largest crack was the shear crack that occurred on the west side, and the width was in the range of 0.04–0.10 mm. The width was 0.12–0.30 mm when converted to the full scale, corresponding to damage class II in Table 1. However, according to the previous research [28], it was assumed that each specimen would reach its maximum strength at R = 0.5%; thus, it can be inferred that the damage class was III.

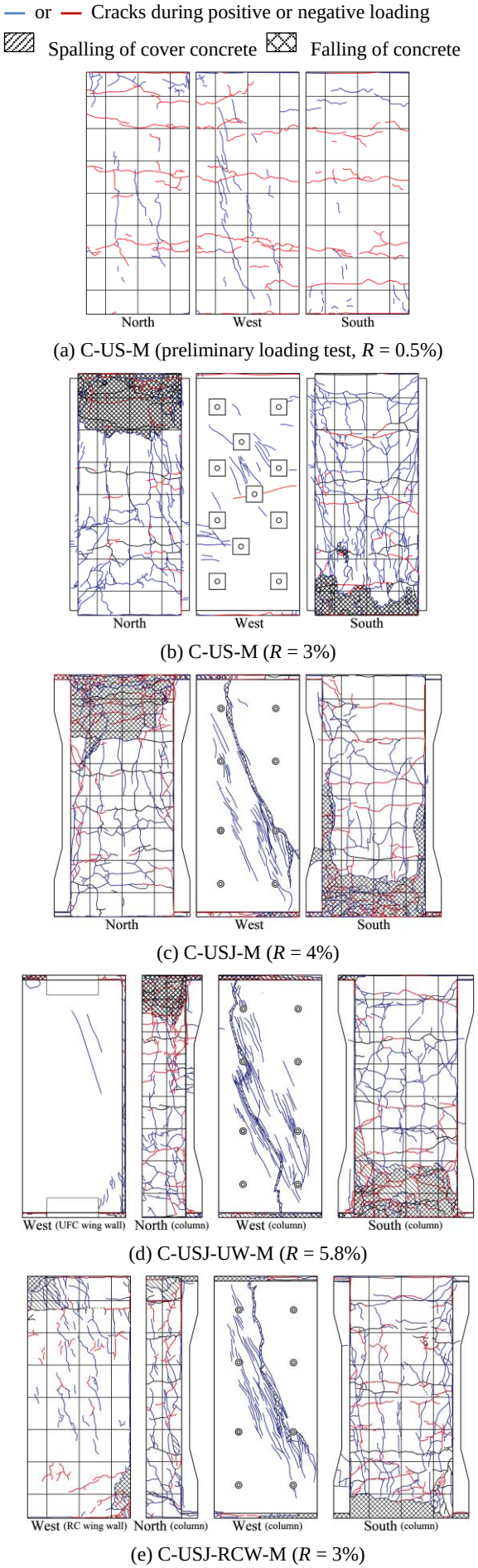

(a) C-US-M (preliminary loading test, R = 0.5%)

(b) C-US-M (R = 3%)

(c) C-USJ-M (R = 4%)

(d) C-USJ-UW-M (R = 5.8%)

(e) C-USJ-RCW-M (R = 3%)

Figure 6: Damage condition at the end of main loading.

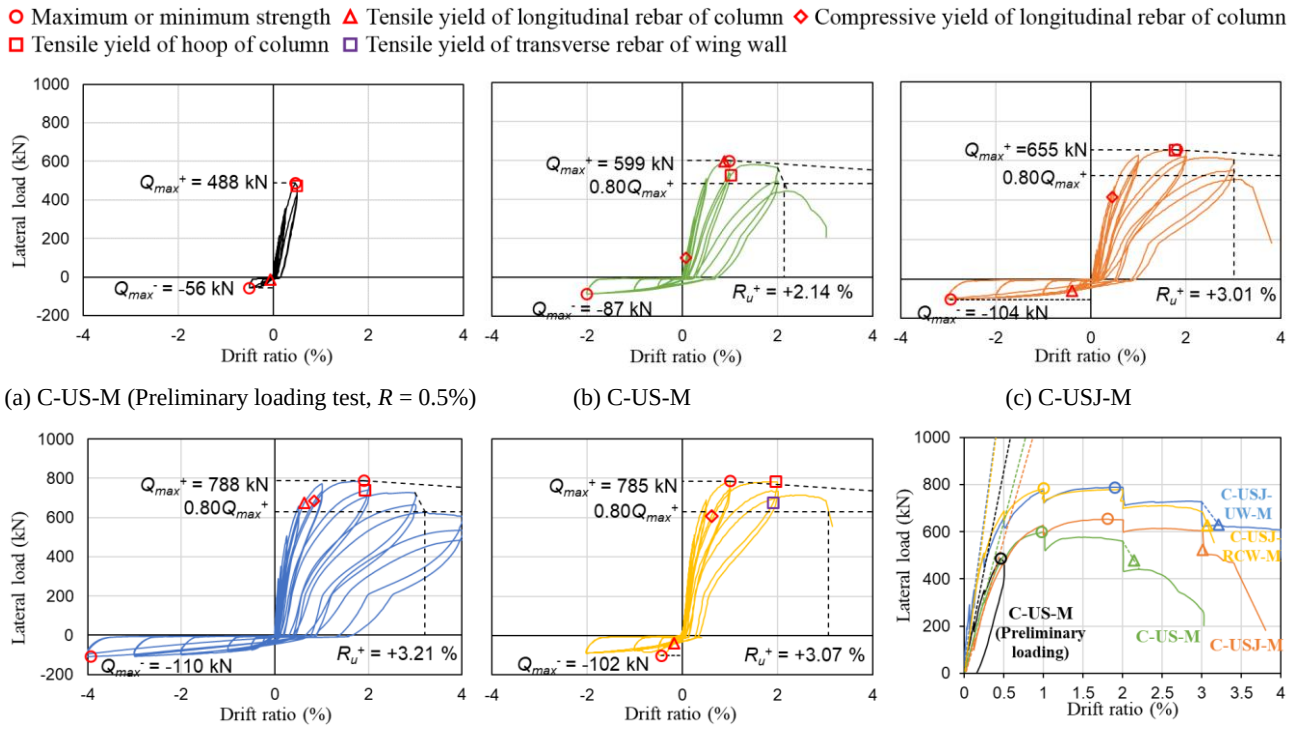

(a) C-US-M (Preliminary loading test, R = 0.5%) (b) C-US-M (c) C-USJ-M

(d) C-USJ-UW-M (e) C-USJ-RCW-M

Figure 7: Lateral load–drift ratio relationship for the main loading.

Figure 8: Envelope curve and initial stiffness.

Main Loading

The flexural cracks that occurred during the preloading on the north and south side of the column were reopened up to R = 0.125% cycle for C-US-M, the R = 0.25% cycle for C-USJ-M and C-USJ-RCW-M, and the R = 0.5% cycle for C-USJ-UW-M. Then, as the drift ratio increased, new cracks occurred.

C-US-M: At the peak of the first cycle of R = +1%, the maximum strength was recorded, and shear cracks were observed in the UFC panel. Horizontal cracks were found in the UFC panel during the first cycle, when R = −1%. During the first cycle to R = +3%, the lateral load decreased considerably, and the concrete on the south side spalled because of the buckling of the longitudinal bars near the bottom of the column. The loading was discontinued because the axial load could not be sustained.

C-USJ-M: The joint mortar between the UFC panel and the stub was partially crushed during the second cycle, when R = 0.5%. At the first cycle to R = +1%, shear cracks occurred in the UFC panel. The maximum strength was recorded during the first cycle to R = +2%. During the first cycle, when R = +4%, the axial collapse occurred because of the shear failure of the UFC panel, and the loading was terminated because the lateral load was reduced considerably.

C-USJ-UW-M: In the first cycle to R = +0.5%, the joint mortar on top and bottom of column and UFC wing wall portions was crushed, and the shear crack occurred in the UFC panel. After measuring the maximum strength near the peak of the first cycle, when R = +2%, the lateral load was decreased. The specimen's strength did not decrease after R = 4% of cyclic loading, and thus, pushover loading was carried out. At approximately R = +5.0%, the shear crack of the UFC panel on the column was greatly widened, and a shear crack also occurred in the UFC wing wall, resulting in a considerable reduction in the lateral load. Near R = +6.0%, the shear cracks of the UFC panel and the UFC wing wall widened, and the joint mortar of the UFC panel and the UFC wing wall was completely crushed. The loading was stopped because further loading would be dangerous.

C-USJ-RCW-M: During the first cycle to R = +0.5%, the joint mortar between the UFC panel and the stub was partially crushed, and many vertical cracks occurred in the RC wing wall. In the first cycle to R = +1%, the mortar on top of the RC wing wall collapsed. Shear cracks occurred in the UFC panel, and the maximal strength was subsequently measured. In the next cycle, the hoop of the RC wing wall yielded in tension at the first cycle to R = +2%. Near the peak of the first cycle to R = +3%, a considerable lateral load degradation accompanied by shear failure of the UFC panel occurred. The axial force could not be maintained; thus, the load was terminated.

Comparison of Experimental Results

Figure 8 depicts the envelope curves (solid lines) and the initial stiffness (dotted lines) of the lateral load–drift ratio relationships for the positive loading direction. Here, circles and triangles indicate the maximum strengths and the ultimate drift ratios, respectively. Table 4 displays the values of the positive maximum strength Q_{max}, ultimate drift ratio R_u, and initial stiffness K_e at the time of preliminary and main loading for each specimen. The ratio for the preloading value of each specimen is indicated in parentheses. The initial stiffness was defined as the secant stiffness that connected the start point of R = +0.03125% cycle and the point of $Q = Q_{max}/3$ on the lateral load–drift ratio relationship curve.

The maximum strength of C-US-M and C-USJ-M was improved by a factor of approximately 1.23 to 1.43 by strengthening with the UFC panels. In contrast, the value of the initial stiffness was 0.76 and 0.54 times that of the preliminary loading, and it did not retain the value of the specimens under the preloading. The maximum strength of C-USJ-UW-M and C-USJ-RCW-M with the UFC or RC wing wall was improved by a factor of 1.58 to 1.66, compared with that of the preloading.

Table 4: Maximum strengths, ultimate drift ratios, and initial stiffness values of tested columns.

Specimen	C-US-M		C-USJ-M		C-USJ-UW-M		C-USJ-RCW-M	
Loading stage	**Preliminary**	**Main**	**Preliminary**	**Main**	**Preliminary**	**Main**	**Preliminary**	**Main**
Maximum strength Q_{max} (kN)	488	599 (1.23)	457	655 (1.43)	500	788 (1.58)	473	785 (1.66)
Ultimate drift ratio R_u (%)	–	2.14	–	3.01	–	3.21	–	3.07
Initial stiffness K_e (kN/mm)	227	172 (0.76)	291	157 (0.54)	288	334 (1.16)	346	339 (0.98)

Table 5: Structural performance of tested columns compared with C-USJ-M.

Specimen	C-US-M	C-USJ-M	C-USJ-UW-M	C-USJ-RCW-M
Maximum strength Q_{max} (kN)	0.91	1.00	1.20	1.20
Ultimate drift ratio R_u (%)	0.71	1.00	1.07	1.02
Initial stiffness K_e (kN/mm)	1.09	1.00	2.12	2.15

The initial stiffness was 0.98 to 1.16 times that of the preliminary loading, which was similar to or slightly higher than the value of the undamaged specimens. This confirmed a notable difference in the initial stiffness improvement by the wing wall. The ultimate drift ratio of all specimens was 2.14%–3.21%, and the ductility of the specimens with joints was better than that of the specimen without joints, C-US-M. The ductility improvement due to the wing wall was insignificant.

For a detailed comparison of the effects according to the strengthening methods, the ratios of the structural performance values of each specimen to those of C-USJ-M are presented in Table 5. As shown in Table 3, it should be noted that there was a difference in the compressive strength and elastic modulus depending on the age of the concrete of the specimens, and C-USJ-M had the lowest compressive strength of the concrete, which was approximately 40.7 N/mm^2. From the comparison of C-US-M and C-USJ-M, the effect of the joint mortar between the stub and the panel was confirmed. Although the concrete compressive strength of C-USJ-M was approximately less than that of C-US-M by 7 N/mm^2, its maximum strength was higher. The ultimate drift ratio of C-US-M was 0.71 times that of C-USJ-M, indicating a considerable difference in deformation performance. The initial stiffness was at an equivalent level considering the difference in the elastic modulus, which further confirmed that the stress was sufficiently transmitted through the epoxy resin adhesive and the post-installed anchor. The maximum strength and initial stiffness of specimens with wing walls for C-USJ-UW-M and C-USJ-RCW-M were higher by factors of approximately 1.20 and 2.12–2.15, respectively. However, the ultimate drift ratio was not considerably different.

EVALUATION OF STRENGTHENING EFFECT

In this chapter, the ultimate flexural and shear strengths of the specimens are calculated to evaluate the strengthening effects. The calculated ultimate strengths are compared with the experimental values. The ultimate strengths are calculated using the method proposed by the authors previously [28]. The experimental values include the maximum load capacity of the specimen, as well as the axial and shear forces of the strengthening members determined through finite element (FE) analysis.

Axial and Shear Force of Strengthening Members during the Experiment

Figure 9 shows the attachment of tri-axial and uni-axial strain gauges to the specimen's strengthening member, which was aimed at estimating the strengthening member's axial force and shear force. The strain gauges attached to the UFC panel of the columns of C-USJ-UW-M and C-USJ-RCW-M were identical to those of C-USJ-M. It was modelled as a quadrilateral element in the FE analysis program FINAL (version 11, ITOCHU Techno-Solutions Corp., Tokyo, Japan) [31] to calculate the stress at each gauge attachment location considering the hysteresis characteristics. At each node of the quadrilateral element, the imposed displacement based on the deformation measured during the experiment was applied.

All the material characteristics of the quadrilateral element corresponded to the previous study [28]. Figure 10 shows the tension-stiffening characteristics of the UFC by "Recommendations for Design and Construction of Ultra High Strength Fiber Reinforced Concrete Structures" [29]. The elastic modulus, compressive strength, and tensile strength of each material were determined according to the results of the material tests in Table 3, and the tensile strength of the mortar was determined using Eq. (2).

$$ {}_mf_t = 1.40\,(\sigma_m/10)^{2/3} \quad (2) $$

where ${}_mf_t$ = tensile strength (N/mm^2); and
σ_m = compressive strength of mortar obtained by the material test, N/mm^2.

Figures 11 and 12 show assumptions of the distributions of axial and shear stresses, respectively, derived from the FE analysis. Linear interpolation was used to estimate the stress values between the measured points. The axial and shear forces were computed by multiplying the stress distribution (represented by the blue area) by the thickness of the strengthening member. In the case of C-US, the shear force was determined by multiplying the average value of the stress distribution by the panel's cross-sectional area, excluding the anchor hole. For the right (south) side of the wing wall in contact with the column, the axial stress was estimated using linear interpolation, and the shear stress was assumed to be equal to that of the adjacent point, as indicated by the dashed line in Figures 11 and 12. On

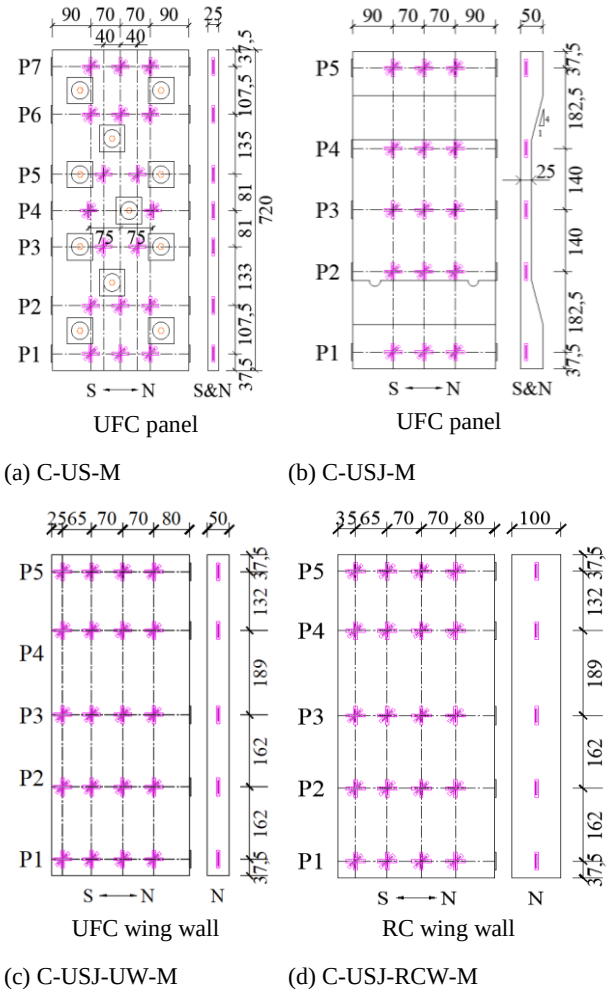

(a) C-US-M (b) C-USJ-M

(c) C-USJ-UW-M (d) C-USJ-RCW-M

Figure 9: Strain gauge attachment positions (unit: mm).

the opposite side of the wing wall and the sides of the UFC panel attached to the column, the shear stress was assumed to be zero. In the following discussions, the axial force in compression is positive, and the positive shear force correspond to the shear force caused by the positive direction of loading.

Comparison of Calculated and Experimental Values

Figure 13 presents the envelope curve of the axial force–drift ratio and shear force–drift ratio relationships for the first loading cycle. The solid black line represents the entire specimen, while the red and blue lines represent the strengthening members determined through FE analysis, the UFC panels on the column and the wing wall, respectively. It depicts the average axial and shear forces of the strengthening member in the middle height cross sections (P2–P6 for C-US-M, P2–P4 for others) in Figure 9. The dashed line represents the drift ratio at the maximum strength of the specimen. In Figure 13, the symbol '*' indicates the points where the specimen and the strengthening member reached their maximum strengths during the loading cycles.

The ultimate flexural and shear strengths of the specimens were calculated using the equations previously proposed by the authors in Appendix A [28]. In the section, the damage caused by the preliminary loading to the column is not considered. The material test results during the main loading presented in Table 3 were used for ultimate strength calculation. It was assumed that the total axial force of the specimen was the target axial compressive force of $0.40bDf'_c$, which was calculated using the compressive strength at preloading.

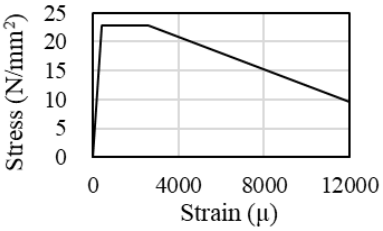

Figure 10: Tension stiffening characteristics of UFC.

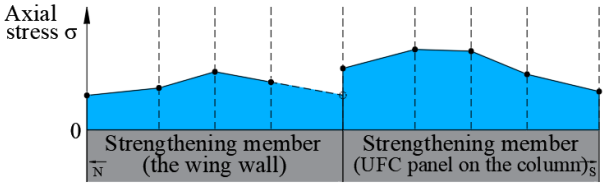

Figure 11: Axial stress distribution assumption [26].

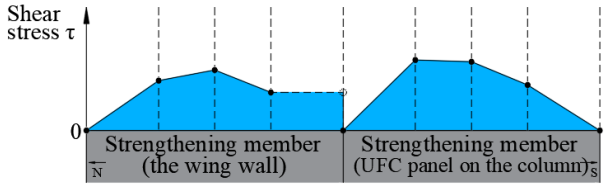

Figure 12: Shear stress distribution assumption [26].

Table 6: Axial forces used for calculating the strengths of the specimens.

Specimen	All (kN)	Column (kN)	UFC panels (kN)	Wing wall (kN)
C-US-M	1995	1995	-	-
C-USJ-M	1667	1277	390	-
C-USJ-UW-M	2007	1281	369	358
C-USJ-RCW-M	1982	1251	353	379

The axial force of each part, e.g., the column, UFC panels, UFC wing wall, and RC wing wall, was calculated according to the elastic axial stiffness of each part. Table 6 presents the axial forces that were used to evaluate the maximum strengths of the specimens. Table 7 shows the calculated ultimate flexural and shear strength of the specimens, along with the maximum load capacity of the specimen measured during the experiment and the corresponding shear forces of the strengthening members determined through FE analysis. The calculated strength with the lowest value is displayed in bold, and the ratio to the experimental value is shown in parentheses. A detailed comparison of the experimental and calculated values of the specimens is presented below.

C-US-M: Because there was no joint mortar between the stub and the UFC panel, the axial force of the UFC panel continued to decrease after the specimen reached the target axial force. The shear force was constant at the drift ratio of 1% when the shear crack was found in the UFC panel, and it decreased at the drift ratio of 2%. The maximum shear force of the UFC panel was 217 kN. The ultimate flexural strength obtained using the cross-sectional analysis was the lowest (516 kN) among the calculated strengths in Table 7, and the experimental value, 599 kN, was higher by a factor of 1.16. The shear strength of 144 kN, which was obtained by multiplying the cross-sectional area

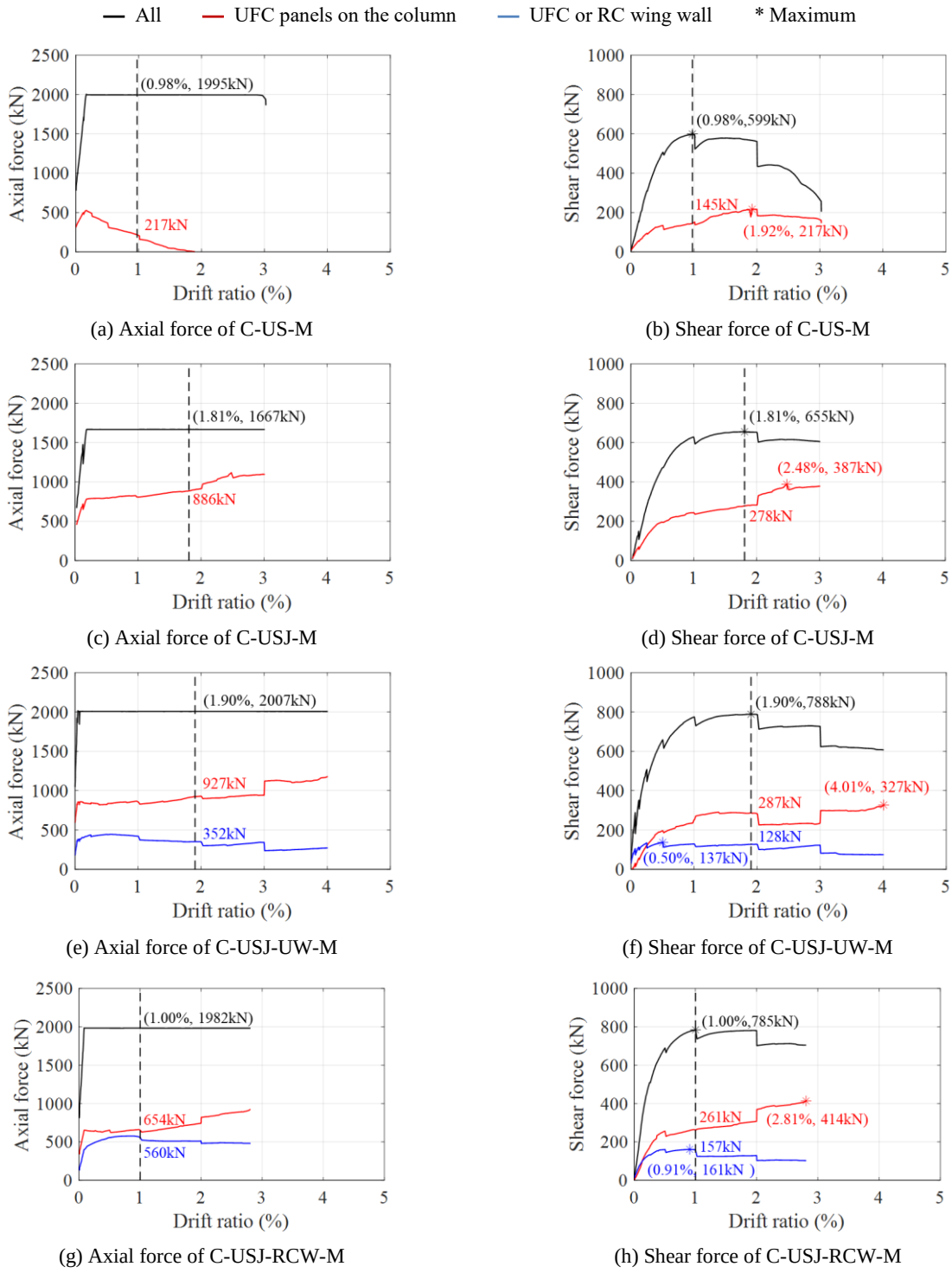

(a) Axial force of C-US-M

(b) Shear force of C-US-M

(c) Axial force of C-USJ-M

(d) Shear force of C-USJ-M

(e) Axial force of C-USJ-UW-M

(f) Shear force of C-USJ-UW-M

(g) Axial force of C-USJ-RCW-M

(h) Shear force of C-USJ-RCW-M

Figure 13: Envelope curves for the 1st positive load in the axial force–drift ratio and shear force–drift ratio relationships.

of the UFC panel excluding the hole for anchor bolts by the UFC shear strength of 12 N/mm^2 [32], was close to the experimental value of 145 kN. When the specimen's maximum strength was recorded at R = 0.98%, the damage situation was shear cracking in the UFC panel. However, the upper and lower ends of the column were severely damaged. It is assumed that C-US-M exhibited the flexural-dominant behaviour mainly because the specimen's strength gradually decreased after the maximum strength was recorded.

C-USJ-M: After the target axial force was reached, the UFC panels retained the same axial force. The shear force of the specimen was 655 kN, which was 1.07 times the ultimate flexural strength of 612 kN considering the fracture of the joint mortar and was the smallest value among those presented in Table 7. The shear force obtained by the strut mechanism for the UFC panels was 298 kN, which was 1.07 times the experimental value of 278 kN. In the damage situation at R = 2% after the specimen's maximum strength was measured, shear cracks increased in the UFC panel and the joint mortar at both ends of the panel was partially crushed. It was presumed that the specimen exhibited flexural-dominant behaviour because the shear force of the UFC panel increased even after cracks developed. The specimen's strength could be displayed steadily once it reaches the maximum strength.

C-USJ-UW-M: The UFC panels attached to the column consistently resisted the axial force throughout the entire cycle. As the drift ratio increased, the axial force of the UFC wing wall decreased slightly. The shear force of the UFC panels declined

Table 7: Comparison of experimental and calculated values.

(1) C-US-M

Part	Experiment (kN)	$_{C\text{-}US}Q_{mu}$ (kN) Simplified method	Cross-sectional analysis	$_{C\text{-}US}Q_{su}$ (kN)
Column + UFC panels	599	554	516 (1.16)	554
UFC panels	145	-	-	144

(2) C-USJ-M

Part	Experiment (kN)	$_{C\text{-}USJ}Q_{mu}$ (kN) No consideration of joint mortar	Consideration of joint mortar	$_{C\text{-}USJ}Q_{su}$ (kN)
Column + UFC panels	655	652	612 (1.07)	633
UFC panels	278	-	-	298

(3) C-USJ-UW-M

Part	Experiment (kN)	$_{C\text{-}USJ}Q_{mu}$ (kN) No consideration of joint mortar	Consideration of joint mortar	$_{C\text{-}USJ}Q_{su}$ (kN)
Column + UFC panels	660	664	631 (1.05)	655
UFC panels	287	-	-	296

	Experiment (kN)	$_{UW}Q_{mu}$ (kN)		$_{UW}Q_{su}$ (kN)	
		No consideration of joint mortar	Consideration of joint mortar	No consideration of joint mortar	Consideration of joint mortar
UFC wing wall	128	127	123 (1.04)	280	243
All	788	754 (1.04)			

(4) C-USJ-RCW-M

Part	Experiment (kN)	$_{C\text{-}USJ}Q_{mu}$ (kN) No consideration of joint mortar	Consideration of joint mortar	$_{C\text{-}USJ}Q_{su}$ (kN)
Column + UFC panels	628	658	629 (1.00)	661
UFC panels	261	-	-	295

	Experiment (kN)	$_{RCW}Q_{mu}$ (kN)	$_{RCW}Q_{su}$ (kN)
RC wing wall	157	114 (1.37)	117
All	785	743 (1.06)	

after R = 2%, which was the cycle at which the specimen's maximum strength was measured. The shear force of the UFC wing wall decreased slightly after its maximum shear force was reached at R = 0.5%. As shown in Table 7, the calculated ultimate strength of the column strengthened with the UFC panels was 631 kN, and the experimental value of 660 kN, was higher by a factor of 1.05. Regarding the damage situation of the UFC panels of the column, after the first shear crack was confirmed at R = 0.5%, the shear crack increased with the drift ratio. There were many shear cracks in the UFC panel at R = 2%. However, the collapse of the bottom of the RC column and the shear failure of the UFC panel occurred with a large drift ratio (approximately R = 5.8%). Therefore, it was assumed that flexural-shear failure occurred in the column strengthened with UFC panels. The flexural strength of the UFC wing wall, considering the joint mortar, was 123 kN, as shown in Table 7. The experimental value of 128 kN was higher than the calculated value by a factor of 1.04. Because there were no cracks in the UFC wing wall at R = 2%, it was determined that the proposed method accurately evaluated the flexural behaviour of the UFC wing wall at the maximum strength of the specimen.

C-USJ-RCW-M: The axial force of the UFC panels attached to the column increased gradually over the entire cycle. Even though the axial force of the RC wing wall decreased slightly after the drift ratio of 1%, but remained stable throughout the entire cycle. The lowest calculated strength of the column part was the ultimate flexural strength of 629 kN, which was close to the experimental value of 628 kN. At R = 1%, where the maximum strength was measured, shear cracks were observed in the UFC panel in the same cycle. The ends of the RC column and the joint mortar were severely damaged. Once the maximum strength was recorded, the shear force of the UFC

panels increased, and the specimen strength remained stable up to R = 2%. Thus, flexural behaviour was presumed to be the dominant mode of the column that was strengthened using UFC panels. Among the calculated values for the RC wing wall, the ultimate flexural strength of 114 kN was the lowest, and the experimental value of 157 kN was higher than the calculated value by a factor of 1.37. The proposed method for evaluating the specimen's strength was appropriate because the damage condition of the RC wing wall exhibited flexural behaviour, as indicated by the partial crushing under compressive force.

EFFECT OF DAMAGE BEFORE STRENGTHENING

The effect of damage to the RC column caused by preliminary loading before strengthening on the structural performance was evaluated. The specimens without preloading (hereinafter, referred to as non-pre-damaged specimens) on the same target column were subjected to the strengthening method using the UFC panel applied in the previous study [28]. The ultimate drift ratio R_u, and the initial stiffness K_e of the non-pre-damaged specimens are listed in Table 8. The ratios of the values for the strengthened specimens after damage (hereinafter, referred to as pre-damaged specimens) to those for the non-pre-damaged specimens for the same strengthening method is also displayed. Regardless of the strengthening method, the ultimate drift ratio R_u of the pre-damaged specimens varied between 1.02–1.50 times that of the non-pre-damaged specimen. The ratio of the initial stiffness K_e of the pre-damaged specimen to the non-pre-damaged specimen was in the range of 0.36–0.58, and it indicates that the pre-damage had a significant effect on the initial stiffness. Because the primary aim of the proposed strengthening method is to restore within a short period, it did not repair cracks or crushing of columns that were caused by preliminary loading. As a result, the stiffness decreases of the column due to damage caused by the preliminary loading was reflected in the initial stiffness of the main loading.

Among the specimens that were strengthened using the same method, there were specimens with substantial differences in concrete compressive strength and elastic modulus depending on the age of the concrete. When comparing the maximum strength of the specimens, the ratio of the experimental value to the calculated ultimate strength was used to account for the variation in concrete compressive strength. Table 9 demonstrates the ratios of experimental values to calculated ultimate strengths for both non-pre-damaged and pre-damaged specimens. The experimental values for non-pre-damaged specimens are presented alongside the ratios. The calculated values for pre-damaged specimens were determined using the concrete compressive strength during the main loading, as indicated in Table 7, without considering the damage to the RC column before strengthening.

For strengthening type C-US, where the calculation assumes that the UFC panel did not resist the axial force, the ratio of the experimental values to ultimate strengths of C-US-M ranged from 1.08 to 1.16, which was close to those of C-US ranging from 1.08–1.17. C-USJ-M had a slight difference in ultimate shear strength compared to C-USJ, but the difference was not notable. Regarding the specimens with wing wall, a noticeable difference between the ratios of wing wall of non-pre-damaged specimens and pre-damaged specimens. The reason is assumed to be the difference of axial force resistance in each portion due to the damage to the RC column. The experimental value divided by the calculated value for the entire specimen was 1.04 for C-USJ-UW-M and 1.06 for C-USJ-RCW-M, which falls within the range of 1.06–1.08 observed in the non-pre-damaged specimens. Therefore, it was assumed that the pre-damage had no significant effect on the specimen's maximum strength. However, further research is required to assess the deterioration in axial stiffness of the specimen caused by the pre-damage to the RC column.

Table 8: Comparison of ultimate drift ratio (R_u) and initial stiffness (K_e) with non-pre-damaged specimen.

Specimen	**C-US**	**C-US-M/ C-US**	**C-USJ**	**C-USJ-M/ C-USJ**
R_u (%)	2.011	1.07	2.005	1.50
K_e (kN/mm)	296	0.58	433	0.36
Specimen	**C-USJ-UW**	**C-USJ-UW-M/ C-USJ-UW**	**C-USJ-RCW**	**C-USJ-RCW-M/ C-USJ-RCW**
R_u (%)	3.013	1.07	3.003	1.02
K_e (kN/mm)	778	0.43	776	0.44

CONCLUSIONS

Four 1/3-scale specimens were subjected to reversed cyclic lateral load tests to determine whether the use of a UFC panel in the RC column strengthening method was adequate for the damaged column. After a preliminary loading of up to 0.5% of the drift ratio that was measured according to the maximum strength of the target column, the specimens were enhanced with UFC panels. The findings of this study are summarized below.

(1) From the comparison of seismic performance before and after strengthening, the maximum strength of the specimens increased by a factor of approximately 1.23–1.66. The ultimate drift ratio of the strengthened specimens was 2.14% for C-US-M, a specimen without joints, and 3.01–3.21% for the other specimens. The effect of the wing wall on the ultimate drift ratio was insignificant compared to C-USJ-M, a specimen without the wing wall. The initial stiffness of the specimens without the wing wall was 0.54–0.76 times before strengthening, and there was no restoration effect for the initial stiffness. The ratio of the initial stiffness of the specimens with the wing wall was approximately 0.98–1.16, which is equivalent to or greater than that of the specimen before strengthening.

(2) The maximum strength and ultimate drift ratio of C-US-M were less than those of C-USJ-M by factors of 0.91 and 0.71, respectively, while the initial stiffness was greater than that of C-USJ-M by a factor of 1.09. It was observed that the stress was adequately transferred to the UFC panel through post-installation anchors and epoxy adhesive. The ultimate drift ratio of specimens with the wing wall differed slightly from C-USJ-M by approximately 1.02–1.07. However, the maximum strength and initial stiffness were 1.20 and 2.12–2.15 times, respectively, confirming the effect of the wing wall on strengthening.

(3) The experimental values of the specimens were compared with the calculated values without considering the damage in the preliminary loading. The smallest value among the calculated ultimate flexural and shear strengths was the ultimate flexural strength for all specimens. The ratios of experimental values to calculated values were 1.00–1.16 for the column strengthened with UFC panels and 1.04–1.35 for the wing wall. All specimens had shear cracks in the UFC panel of the column when their maximum strength was measured. It was assumed, however, that they exhibited flexural-dominant behaviour because the upper and lower ends of the column were severely damaged, and the load capacity of all specimens gradually decreased.

(4) The ultimate drift ratio, initial stiffness, and maximum strength of pre-damaged and non-pre-damaged specimens with the same target column and strengthening method were compared. The ultimate drift ratio was 1.02–1.07

Table 9: Ratios of experimental value to calculated value of non-pre-damaged and pre-damaged specimens.

Specimen		**C-US**				**C-US-M**			
Part	Experiment (kN)	$_{C\text{-}US}Q_{mu}$ Simplified method	Cross-sectional analysis	$_{C\text{-}US}Q_{su}$		$_{C\text{-}US}Q_{mu}$ Simplified method	Cross-sectional analysis	$_{C\text{-}US}Q_{su}$	
Column + UFC panels	589	1.08	1.17	1.08		1.08	1.16	1.08	
Specimen	**C-USJ**					**C-USJ-M**			
Part	Experiment (kN)	$_{C\text{-}USJ}Q_{mu}$ ①	②	$_{C\text{-}USJ}Q_{su}$		$_{C\text{-}USJ}Q_{mu}$ ①	②	$_{C\text{-}USJ}Q_{su}$	
Column + UFC panels	729	1.03	1.10	1.09		1.01	1.07	1.03	
Specimen	**C-USJ-UW**					**C-USJ-UW-M**			
Part	Experiment (kN)	$_{C\text{-}USJ}Q_{mu}$ ①	②	$_{C\text{-}USJ}Q_{su}$		$_{C\text{-}USJ}Q_{mu}$ ①	②	$_{C\text{-}USJ}Q_{su}$	
Column + UFC panels	601	0.97	1.02	0.94		0.99	1.05	1.01	
	Experiment (kN)	$_{UW}Q_{mu}$ ①	②	$_{UW}Q_{su}$ ①	②	$_{UW}Q_{mu}$ ①	②	$_{UW}Q_{su}$ ①	②
UFC wing wall	142	1.20	1.24	0.51	0.61	1.01	1.04	0.46	0.53
All	743	1.06				1.04			
Specimen	**C-USJ-RCW**					**C-USJ-RCW-M**			
Part	Experiment (kN)	$_{C\text{-}USJ}Q_{mu}$ ①	②	$_{C\text{-}USJ}Q_{su}$		$_{C\text{-}USJ}Q_{mu}$ ①	②	$_{C\text{-}USJ}Q_{su}$	
Column + UFC panels	701	1.03	1.08	1.05		0.95	1.00	0.95	
	Experiment (kN)	$_{RCW}Q_{mu}$		$_{RCW}Q_{su}$		$_{RCW}Q_{mu}$		$_{RCW}Q_{su}$	
RC wing wall	135	1.10		1.11		1.37		1.34	
All	836	1.08				1.06			

Note: The concrete compressive strengths of the C-US, C-USJ, C-USJ-UW, the column of C-USJ-RCW, and the wing wall of C-USJ-RCW were 46.7, 46.2, 44.9, 51.6, and 50.6 N/mm^2, respectively. Other material test results are listed in [26].

① means no consideration of joint mortar and ② means consideration of joint mortar.

times that of the non-pre-damaged specimens, except for the case of C-USJ-M, wherein the value was 1.5 times that of C-USJ. On the other hand, damage before strengthening notably reduced the initial stiffness by a factor of 0.36–0.58. Regarding the maximum strength, the ratio of the experimental value to the calculated value was compared in order to consider the difference in concrete compressive strength. The ratios of C-US-M were nearly identical to those of C-US. When comparing C-USJ and C-USJ-M, there was a slight difference in the ratio for ultimate shear strength but the difference was not notable. In the case of specimens with wing walls, the experimental value divided by the calculated value for entire specimen was 1.04-1.06, which was comparable to the value of 1.06–1.08 for non-pre-damaged specimens. Consequently, the effect of pre-damage on the maximum strength was minimal.

(5) However, there is an observable difference in the wing wall ratios between non-pre-damaged and pre-damaged specimens in the case of specimens with the wing wall. The cause is assumed to be a difference in axial force resistance in each portion, resulting from the pre-damage to the RC column.

ACKNOWLEDGMENTS

This research study was based on the "Promotion of emergency response by quick preparation of temporary/reconstruction housing" (PD: Mitsumasa Midorikawa) of "Public/Private R&D Investment Strategic Expansion PrograM (PRISM)" for the Innovative Construction/Infrastructure Maintenance Technology/Innovative Disaster Prevention · Disaster Mitigation Technology (Director: Tamiharu Tashiro), and the research project was designated by the Building Research Institute as part of "Development of seismic resistance evaluation technology for continuous use of existing buildings after an earthquake." This research was also financially supported by JSPS KAKENHI, Grant Numbers JP21J14758 (Principal Investigator: M. Nishiyama), and was supported by the National University Development Project by the Ministry of Education in 2023. The authors also express their appreciation to Taiheiyo Cement Co., Ltd., Mitsubishi Chemical Infratec Co., Ltd., Masahiro Nomura, a technical staff member of Kyoto University, Rei Ishihara, a former graduate student of Kyoto University, and Haruka Yoshida, a graduate student of Kyoto University, for their cooperation in this research effort.

REFERENCES

1 Earthquake Engineering Research Institute (2003). "*Preliminary Observations on the October 31-November 1, 2002 Molise, Italy, Earthquake Sequence*". EEEI Special Earthquake Report — January 2003, EERI, Oakland, CA. https://www.eeri.org/lfe/pdf/italy_molise_eeri_report.pdf

2 Japan Meteorological Agency (Retrieved 2022). "*2016 Kumamoto Earthquake Information*". https://www.data.jma.go.jp/svd/eqev/data/2016_04_14_kumamoto/index.html

3 Sarrafzadeh M, Elwood KJ, Dhakal RP, Ferner H, Pettinga D, Stannard M, Maeda M, Nakano Y, Mukai T and Koike T (2017). "Performance of reinforced concrete buildings in the 2016 Kumamoto earthquakes and seismic design in Japan". *Bulletin of the New Zealand Society for Earthquake Engineering*, **50**(3): 394-435. https://doi.org/10.5459/bnzsee.50.3.394-435

4 Filippova O, Elwood K and Collins T (2023). "Challenges in post-earthquake recovery of damaged and neglected buildings in Christchurch CBD". *Bulletin of the New Zealand Society for Earthquake Engineering*, **56**(1): 38-54. https://doi.org/10.5459/bnzsee.56.1.38-54

5 Moretti ML, Miliokas E and Paparizos I (2022). "Retrofit of damaged RC columns using CFRP Jackets". *10th International Conference on FRP Composites in Civil Engineering*, 8-10 December, İstanbul, 1229-1240. https://doi.org/10.1007/978-3-030-88166-5_107

6 Karadogan HF (2007). "Local thin jacketing for the retrofitting of reinforced concrete columns". *Structural Engineering and Mechanics*, **27**: 589-607. https://doi.org/10.12989/sem.2007.27.5.589

7 Ma G and Li H (2015). "Experimental study of the seismic behavior of predamaged reinforced-concrete columns retrofitted with basalt fiber–reinforced polymer". *Journal of Composites for Construction*, **19**: 04015016. https://doi.org/10.1061/(ASCE)CC.1943-5614.0000572

8 Ghoroubi R, Mercimek Ö, Özdemir A and Anil Ö (2020). "Experimental investigation of damaged square short RC columns with low slenderness retrofitted by CFRP strips under axial load". *Structures*, **28**: 170-180. https://doi.org/10.1016/j.istruc.2020.08.068

9 Memon MS and Sheikh SA (2005). "Seismic resistance of square concrete columns retrofitted with glass fiber-reinforced polymer". *ACI structural journal*, **102**: 774. https://doi.org/10.14359/14673

10 Wang H, Xing G, Zhao J and Wen F (2022). "Seismic behavior of RC columns strengthened with near-surface-mounted aluminum alloy bars and CFRP wraps". *Engineering Structures*, **268**: 114742. https://doi.org/10.1016/j.engstruct.2022.114742

11 Janwaen W, Barros JA and Costa IG (2019). "A new strengthening technique for increasing the load carrying capacity of rectangular reinforced concrete columns subjected to axial compressive loading". *Composites Part B: Engineering*, **158**: 67-81. https://doi.org/10.1016/j.compositesb.2018.09.045

12 Xing L, Lin G and Chen J (2020). "Behavior of FRP-confined circular RC columns under eccentric compression". *Journal of Composites for Construction*, **24**: 04020030. https://doi.org/10.1061/(ASCE)CC.1943-5614.0001036

13 Zeng J, Lin G, Teng J and Li L (2018). "Behavior of large-scale FRP-confined rectangular RC columns under axial compression". *Engineering Structures*, **174**: 629-645. https://doi.org/10.1016/j.engstruct.2018.07.086

14 Pohoryles DA, Melo J, Rossetto T, Varum H and Bisby L (2019). "Seismic retrofit schemes with FRP for deficient RC beam-column joints: State-of-the-art review". *Journal of Composites for Construction*, **23**: 03119001. https://doi.org/10.1061/(ASCE)CC.1943-5614.0000950

15 Attari N, Youcef YS and Amziane S (2019). "Seismic performance of reinforced concrete beam–column joint strengthening by frp sheets". *Structures*, **20**: 353-364. https://doi.org/10.1016/j.istruc.2019.04.007

16 Parthasarathy A and Vidjeapriya R (2022). "Behaviour of retrofitted beam column joints under monotonic and cyclic loading- A review". *Materials Today: Proceedings*, **65**: 1726-1738. https://doi.org/10.1016/j.matpr.2022.04.772

17 Ceroni F (2010). "Experimental performances of RC beams strengthened with FRP materials". *Construction and Building materials*, **24**: 1547-1559. https://doi.org/10.1016/j.conbuildmat.2010.03.008

18 Chen C, Wang X, Sui L, Xing F, Chen X and Zhou Y (2019). "Influence of FRP thickness and confining effect on flexural performance of HB-strengthened RC beams". *Composites Part B: Engineering*, **161**: 55-67. https://doi.org/10.1016/j.compositesb.2018.10.059

19 Ilkhani M, Naderpour H and Kheyroddin A (2021). "Experimental investigation on behavior of FRP-strengthened RC beams subjected to combined twisting-bending moments". *Engineering Structures*, **242**: 112617. https://doi.org/10.1016/j.engstruct.2021.112617

20 Xue J, Lavorato D, Fiorentino G, Bergami AV, Briseghella B and Nuti C (2022). "FRP reinforcement to retrofit bridge pier after repair: experimental test results". *10th International Conference on FRP Composites in Civil Engineering*, December 8-10, İstanbul, 449-458. https://doi.org/10.1007/978-3-030-88166-5_38

21 Fahmy MF and Wu Z (2018). "Restoration of pre-damaged RC bridge columns using basalt FRP composites". *Earthquakes and Structures*, **14**: 379-388. https://doi.org/10.12989/eas.2018.14.5.379

22 Cheng C-T, Mo Y and Yeh Y-K (2005). "Evaluation of as-built, retrofitted, and repaired shear-critical hollow bridge columns under earthquake-type loading". *Journal of Bridge Engineering*, **10**: 520-529. https://doi.org/10.1061/(ASCE)1084-0702(2005)10:5(520)

23 Sugano S, Kimura H and Shirai K (2007). "Study of new RC structures using ultra-high-strength fiber-reinforced concrete (UFC)-the challenge of applying 200 MPa UFC to earthquake resistant building structures". *Journal of Advanced Concrete Technology*, **5**: 133-147. https://doi.org/10.3151/jact.5.133

24 Uchida Y, Takeyama T and Dei T (2010). "Ultra high strength fiber reinforced concrete using aramid fiber". *Proceedings of FraMCoS-7*, 23 May, Jeju, South Korea, 1492-1496. http://www.framcos.org/FraMCoS-7/12-16.pdf

25 Kumabe A, Tani M, Mukai T, Watanabe H, Nishiyama M, Ishioka T, Hattori T, Matsumoto D and Hori S (2021). "Cyclic loading tests on damaged R/C soft-first story columns retrofitted by sandwiching and bonding UFC panels". *AIJ Journal of Technology and Design*, **27**: 1273-1278. [in Japanese]. https://doi.org/10.3130/aijt.27.1273

26 Japan Building Disaster Prevention Association (JBDPA) (2015). "*Guidelines for Post-Earthquake Damage Evaluation and Rehabilitation of RC Buildings*". Japan Building Disaster Prevention Association, Tokyo. [in Japanese].

27 Nakano Y, Maeda M, Kuramoto H and Murakami M (2004). "Guideline for post-earthquake damage evaluation and rehabilitation of RC buildings in Japan". *13th World Conference on Earthquake Engineering*, August 1-6, Vancouver, B.C., Canada, 124. http://sismo.iis.u-tokyo.ac.jp/Research.files/pp/rsd3.pdf

28 Lim SA, Tani M, Watanabe H, Mukai T, Nishimura E, Hori S, Matsumoto D and Nishiyama M (2023). "Strengthening method by using ultra-high-strength fiber-reinforced concrete panels for a column on the soft first story of a reinforced concrete building". *Engineering Structures*, **278**: 115468. https://doi.org/10.1016/j.engstruct.2022.115468

29 Japan Society of Civil Engineers (2004). "*Recommendations for Design and Construction of Ultra-High Strength Fiber Reinforced Concrete Structures-Draft- (Concrete Library 113)*". Japan Society of Civil Engineers, Tokyo. [in Japanese].

30 Japan Building Disaster Prevention Association (JBDPA) (2001). "*Standard for Seismic Evaluation of Existing Reinforced Concrete Buildings*". Japan Building Disaster Prevention Association, Tokyo.

31 Itochu Techno-Solutions Co. L "FINAL/V11".

32 Mukai T, Fukuyama H, Suwada H, Shirai K and Kinugasa H (2015). "Ultimate strength of R/C column retrofitted by precast wing walls with ultra high strength fiber reinforced concrete". *Journal of Structural and Construction Engineering*, **80**: 637-645. [in Japanese]. https://doi.org/10.3130/aijs.80.637

APPENDIX A

The ultimate flexural strength of C-US based on the simplified method is given as follows:

(i) $N_{min} \le N < 0$ (A1-a)

$$_{C-US}M_u = 0.5a_g\sigma_y g_1 D + 0.5Ng_1 D$$

(ii) $0 \le N < N_b$

$$_{C-US}M_u = 0.5a_g\sigma_y g_1 D + 0.5ND\left(1-\frac{N}{bDf'_c}\right)$$

(iii) $N_b \le N < N_{max}$

$$_{C-US}M_u = \left\{0.5a_g\sigma_y g_1 D + 0.024(1+g_1)(3.6-g_1)bD^2 f'_c\right\}\left(\frac{N_{max}-N}{N_{max}-N_b}\right)$$

where $_{C\text{-}US}M_u$ = ultimate flexural strength (N·mm);
N = axial force (N);
N_{min} = axial tensile strength (= $-a_g\sigma_y$, N);
N_b = axial force in the balanced failure case (= $0.22(1 + g_1)bDf'_c$, N);
N_{max} = axial compressive strength (= $bDf'_c + a_g\sigma_y$, N);
D = depth of the column (mm);
b = width of the column (mm);
f'_c = compressive strength of concrete (N/mm^2);
a_g = total cross-sectional area of the reinforcing bars (mm^2);
σ_y = yield strength of reinforcing bars (N/mm^2); and
g_1 = ratio of the distance between the center of the tensile rebar and the center of the compressive rebar to the D (decimal).

The ultimate flexural strength of C-US based on the section analysis method is given as follows:

$$_{C-US}M_u = \sum T_{si}d_{si} - \sum C_{si}d_{si} - C_c\beta_1 x_n / 2 + ND/2 \quad \text{(A1-b)}$$

where $_{C\text{-}US}M_u$ = ultimate flexural strength of C-US (N·mm);
T_{si} = tensile force of each tensile reinforcing bar (N);
d_{si} = distance from the extreme compression fiber to each reinforcing bar (mm);
C_{si} = compressive force of the compressed reinforcing bar (N);
C_c = compressive force of concrete (= $0.85f'_cab$, N);
a = depth of equivalent rectangular stress block (mm) and $a = \beta_1 x_n$;, mm);
β_1 = factor related depth of equivalent rectangular compressive stress block to the neutral axis depth (when $f'_c \le 28$ N/mm^2, $\beta_1 = 0.85$, and when $f'_c > 28$ N/mm^2, $\beta_1 = 0.85 - 0.05(f'_c - 28)/7 \ge 0.65$); and
x_n = depth to neutral axis (mm).

The shear strength at the ultimate flexural strength of C-US is given as follows:

$$_{C-US}Q_{mu} = 2\,_{C-US}M_u / h_0 \quad \text{(A1-c)}$$

where $_{C\text{-}US}Q_{mu}$ = shear strength at the ultimate flexural strength of C-US (N); and
h_0 = clear height of the specimen (mm).

The ultimate shear strengths of C-US and UFC panels are given by

$$_{C-US}Q_{su} = {}_{C}Q_{su} + {}_{US}Q_{su} \quad \text{(A2-a)}$$

$${}_{C}Q_{su} = \left\{\frac{0.068p_t^{0.23}(f'_c+18)}{M/(Qd)+0.12} + 0.85\sqrt{p_w\sigma_{wy}} + 0.1\sigma_0\right\}bj \quad \text{(A2-b)}$$

$${}_{US}Q_{su} = \tau_{ufc}A_{us} \quad \text{(A2-c)}$$

where $_{C\text{-}US}Q_{su}$, $_{C}Q_{su}$ and $_{US}Q_{su}$ = ultimate shear strengths of C-US, the RC column, and UFC panels, respectively (N);
p_t = tensile reinforcement ratio (tensile rebar is defined as the second bar from the end, %);
M/Q = shear span length (mm);
d = effective depth of column (mm);
$M/(Qd)$ = shear span-to-effective depth ratio (when $M/(Qd) \le 1$, $M/(Qd) = 1$ and when $M/(Qd) \ge 3$, $M/(Qd) = 3$);
p_w = shear reinforcement ratio, ($p_w = 0.012$ for $p_w \ge 0.012$, decimal);
σ_{wy} = yield strength of shear reinforcing bars (N/mm^2);
σ_0 = axial stress in the column (= $N/(bD)$, When $\sigma_0 \ge 0.4f'_c$, $\sigma_0 = 0.4f'_c$, N/mm^2);
j = distance between the centroids of tension and compression forces (=7d/8, mm);
τ_{ufc} = shear strength of UFC (12 N/mm^2); and
A_{us} = total cross-sectional area of UFC panels (mm^2).

The shear strength at the ultimate flexural strength of C-USJ is given by

$$_{C-USJ}M_u = \sum T_{si}d_{si} - \sum C_{si}d_{si} - C_c\beta_1 x_n / 2 - C_{us}x_n / 3 + ND/2 \quad \text{(A3-a)}$$

$$_{C-USJ}Q_{mu} = 2\,_{C-USJ}M_u / h_0 \quad \text{(A3-b)}$$

where $_{C\text{-}USJ}M_u$ = ultimate flexural strength of C-USJ (N·mm);
C_{us} = compressive force of the UFC panels ($C_{us} = 2t_{us}'\varepsilon_{cu}E_{ufc}x_n/2$, when the UFC was elastic, and $C_{us} = 2t_{us}'\varepsilon_{cu}E_m x_n/2$ when the joint mortar was elastic, N);
t_{us}' = thickness of the end of the panel (mm);
ε_{cu} = extreme compression fiber (= 0.003);
E_m = Young's modulus of the joint mortar (N/mm^2); and
$_{C\text{-}USJ}Q_{mu}$ = shear strength at the ultimate flexural strength of C-USJ (N).

The ultimate shear strengths of C-USJ and UFC panels are given by

$$_{C-USJ}Q_{su} = {}_{C}Q_{su} + {}_{USJ}Q_{su} \quad \text{(A4-a)}$$

$$_{USJ}Q_{su} = 0.5\nu_0\sigma_{ufc}\,2t_{us}x_n\sin 2\theta \quad \text{(A4-b)}$$

$$x_n = \frac{D}{4}(1+2\eta) \quad \text{(A4-c)}$$

$$\theta = \tan^{-1}\frac{D-x_n}{L}\times\frac{\pi}{180} \quad \text{(A4-d)}$$

where $_{C\text{-}USJ}Q_{su}$ and $_{USJ}Q_{su}$ = ultimate shear strengths of C-USJ and UFC panels, respectively (N);
ν_0 = effective strength factor (ν_0 = 1.0);
σ_{ufc} = compressive strength of UFC (N/mm^2);
t_{us} = thickness of the middle part of a UFC panel (mm);
x_n = neutral axial depth of the UFC panel (mm);
η = axial ratio of UFC panels ($\eta = N_{us}/(t_{us}D\sigma_{ufc})$, decimal);
θ = angle of the strut mechanism (rad); and
D and L are the depth and length of the UFC panel, respectively (mm).

The shear strengths at the ultimate flexural strength of C-USJ-UW and the UFC wing wall are as follows:

$$_{C-USJ-UW}Q_{mu} = {}_{C-USJ}Q_{mu} + {}_{UW}Q_{mu} \quad \text{(A5-a)}$$

$$_{UW}Q_{mu} = ({}_{UW}M_{ut} + {}_{UW}M_{ub})/h_0 \quad \text{(A5-b)}$$

$$_{UW}M_{ut} = C_{uw}(D_{uw} - {}_{uw}x_n/3) + N_{uw}D/2 \quad \text{(A5-c)}$$

$$_{UW}M_{ub} = -C_{uw}(D + {}_{uw}x_n/3) + N_{uw}D/2 \quad \text{(A5-d)}$$

$$C_{uw} = N_{uw} = \frac{1}{2}\sigma_{ufc}\,{}_{uw}x_n\,t_{uw} \quad \text{or} \quad C_{uw} = N_{uw} = \frac{1}{2}\sigma_{mc}\,{}_{uw}x_n\,t_{uw} \quad \text{(A5-e)}$$

$$\sigma_{mc} = \sigma_m + 69\left(1 - l/\left(\sqrt{3}t_{uw}\right)\right)\left(1 - l/\left(\sqrt{3}D_{uw}\right)\right) \quad \text{(A5-f)}$$

where $_{C\text{-}USJ\text{-}UW}Q_{mu}$ and $_{UW}Q_{mu}$ = shear strengths at the ultimate flexural strength of C-USJ-UW and the UFC wing wall, respectively (N);
$_{UW}M_{ut}$ and $_{UW}M_{ub}$ = ultimate flexural moments of the upper and lower ends of the UFC wing wall (N·mm);
C_{uw} = compressive force of the UFC wing wall (N);
D_{uw} = depth of the UFC wing wall (mm);
$_{uw}x_n$ = neutral axis depth of the UFC wing wall (mm);
t_{uw} = thickness of the UFC wing wall (mm);
σ_{mc} = compressive strength of the joint mortar when the constraint area is considered (N/mm^2);
σ_m = compressive strength of the joint mortar (N/mm^2); and
l = height of the joint mortar (mm).

The ultimate shear strength of C-USJ-UW can be expressed as

$$_{C-USJ-UW}Q_{su} = {}_{C-USJ}Q_{su} + {}_{UW}Q_{su} \quad \text{(A6-a)}$$

$$_{UW}Q_{su} = 0.5\nu_0\,\sigma_{ufc}\,t_{uw}\,{}_{uw}x_n\sin 2\theta \quad \text{(A6-b)}$$

$$_{uw}x_n = \frac{D_{uw}}{4}(1+2\eta) \quad \text{(A6-c)}$$

$$\theta = \tan^{-1}\frac{D_{uw} - {}_{uw}x_n}{L_{uw}}\times\frac{\pi}{180} \quad \text{(A6-d)}$$

where, $_{C\text{-}USJ\text{-}UW}Q_{su}$ = ultimate shear strength of C-USJ-UW (N);
$_{C\text{-}USJ}Q_{su}$ and $_{UW}Q_{su}$ = shear strengths of the column strengthened with UFC panels and a UFC wing wall, respectively (N);
t_{uw} = thickness of the UFC wing wall (mm); and
$_{uw}x_n$ = neutral axial depth of the UFC wing wall, which is identical to C-USJ (mm).

The shear strengths at the ultimate flexural strength of C-USJ-RCW and the RC wing wall are as follows:

$$_{C-USJ-RCW}Q_{mu} = {}_{C-USJ}Q_{mu} + {}_{RCW}Q_{mu} \quad \text{(A7-a)}$$

$$_{RCW}Q_{mu} = ({}_{RCW}M_{ut} + {}_{RCW}M_{ub})/h_0 \quad \text{(A7-b)}$$

$$_{RCW}M_{ut} = C_{rcw}(D_{rcw} - \beta_1{}'_{rcw}x_n/2) + N_{rcw}D/2 \quad \text{(A7-c)}$$

$$_{RCW}M_{ub} = -C_{rcw}(D + \beta_1{}'_{rcw}x_n/2) + N_{rcw}D/2 \quad \text{(A7-d)}$$

$$C_{rcw} = N_{rcw} = 0.85_{rcw}f'_c\,\beta_1{}'_{rcw}x_n\,t_{rcw} \quad \text{(A7-e)}$$

where $_{C\text{-}USJ\text{-}RCW}Q_{mu}$ and $_{RCW}Q_{mu}$ = shear strengths at the ultimate flexural strength of C-USJ-RCW and the RC wing wall, respectively (N);
$_{RCW}M_{ut}$ and $_{RCW}M_{ub}$ = ultimate flexural moments of the upper and lower ends of the RC wing wall (N·mm);
C_{rcw} = compressive force of the RC wing wall (N);
D_{rcw} = depth of the RC wing wall (mm);
β_1' = factor relating depth of equivalent rectangular compressive stress block to the neutral axis depth of the RC wing wall (when $f'_c \le 28$ N/mm^2, $\beta_1' = 0.85$, and when $f'_c >$ 28N/mm^2, $\beta_1' = 0.85 - 0.05(_{rcw}f'_c - 28)/7 \ge 0.65$);
$_{rcw}x_n$ = neutral axis depth of the RC wing wall (mm);
t_{rcw} = thickness of the RC wing wall (mm); and
$_{rcw}f'_c$ = concrete compressive strength of the RC wing wall (N/mm^2).

The ultimate shear strength of the C-USJ-RCW can then be expressed as

$$_{C-USJ-RCW}Q_{su} = {}_{C-USJ}Q_{su} + {}_{RCW}Q_{su} \quad \text{(A8-a)}$$

$$_{RCW}Q_{su} = \left\{\frac{0.068\,{}_{rcw}p_t^{0.23}({}_{rcw}f'_c + 18)}{(M/Q)_{rcw}/d_{rcw} + 0.12} + 0.85\sqrt{{}_{rcw}p_w \times {}_{rcw}\sigma_{wy}} + 0.1\,{}_{rcw}\sigma_0\right\} t_{rcw}j_{rcw} \quad \text{(A8-b)}$$

where $_{C\text{-}USJ\text{-}RCW}Q_{su}$ = ultimate shear strength of the C-USJ-RCW (N);
$_{C\text{-}USJ}Q_{su}$ and $_{RCW}Q_{su}$ = ultimate shear strengths of the column strengthened with the UFC panels and the RC wing wall, respectively (N);
$_{rcw}p_t$ = tensile reinforcement ratio (%);
$(M/Q)_{rcw}$ = shear span length of the RC wing wall (mm);
d_{rcw} = effective depth of the RC wing wall (mm);
$_{rcw}p_w$ = shear reinforcement ratio of the RC wing wall (decimal);
$_{rcw}\sigma_{wy}$ = yield strength of shear reinforcing bars of the RC wing wall (N/mm^2);
$_{rcw}\sigma_0$ = axial stress in the RC wing wall (= N_{rcw}/A_{rcw}, N/mm^2, A_{rcw} = cross-sectional area of the RC wing wall, mm^2); and
j_{rcw} = distance between the centroids of the tensile and compressive forces (= 7/8d_{rcw}, mm).